

Stopping power and nano-particles: Collisions of ions in low charge states with metallic clusters

T. Bergen, A. Brenac, F. Chandezon, C. Guet, H. Lebius, A. Pesnelle, and B.A. Huber^a

Département de Recherche Fondamentale sur la Matière Condensée, GIM, CEA-Grenoble, 17 rue des Martyrs, 38054 Grenoble Cedex 9, France

Received 8 November 2000 and Received in final form 26 January 2001

Abstract. In an experimental study, the multi-ionisation of metallic clusters (Na_n) has been analysed in collisions with light ions in low charge states (H^+ , He^+ , He^{2+} , O^{3+}) at collision velocities below 1 a.u. Cluster ions are produced in charge states up to 5+. The average charge of the nano-particles is found to increase linearly with the variation of projectile velocity and the square of the effective projectile charge, well in agreement with the electronic stopping power of the bulk material. A fraction of 50% to 30% of the total projectile energy loss (decreasing with velocity) is transferred into vibrational modes in good agreement with recent theoretical predictions.

PACS. 36.40.Wa Charged clusters – 34.50.Bw Energy loss and stopping power

1 Introduction

Multi-ionisation of metal clusters induced by ions in low charge states (in the extreme case singly charged ions) requires collisions with small impact parameters, where the projectile is likely to penetrate the metal cluster. In the present velocity range (0.2 to 0.8 a.u.) such collisions are characterised by an electronic interaction. The penetrating charge is shielded by the delocalised valence electrons of the cluster and provokes, therefore, a strong perturbation of the electron density distribution. In terms of the stopping power concept [1,2], which has been developed to describe the interaction of ions with extended solids, this means that the electronic stopping power well dominates over the nuclear one which is due to elastic heavy particle collisions.

In recent years several studies have been performed concerning the interaction of ions with metal clusters [3–8] and very thin carbon foils [9]. In this context the projectile energy loss, the cluster excitation, the electron emission and the charge equilibration during the passage as well as effects due to the finite size of nano-particles have been addressed. Concerning low-charged projectiles [3–5], these studies have shown that when entering the metal cluster the projectile charge will be strongly screened by the target electrons, thus causing a strong perturbation of the electron density distribution. This deformation is asymmetric with respect to the position of the projectile and the size of the perturbed region increases with increasing projectile velocity. Due to this collective electronic excitation the projectile loses in a monotone fashion

kinetic energy during the passage. When passing and leaving the cluster, the projectile charge attracts several electrons which try to follow with similar velocities and directions, leading to a instantaneous multi-ionisation of the cluster. Recently, the thermal emission of electrons on a much longer time scale (100 fs, emitted by a hot electron gas) has been studied in fs-laser experiments [10]. However, for ion collisions the perturbation by the incoming charge is much shorter and has a different character. Therefore, the theoretical predictions [3–5] indicate in the present case that a delayed emission is less important.

Finite size effects, *i.e.* a behaviour which differs from that of an infinitely extended target, might be expected as soon as the size of the perturbation equals the diameter of the cluster, which implies velocities higher than those studied in the present contribution. In an extended solid an equilibrium charge state of the incoming projectile is obtained, which is normally used to calculate energy losses of ions in solids. This is not as clear for clusters with a limited size. Recent experiments [9] with very thin carbon foils (thickness of 5–10 nm) have shown, that for collisions of Xe^{44+} or Au^{68+} ($v = 0.5$ a.u.) the charge state distributions are not yet in the equilibrium state. A charge equilibration time of about 7 fs has been determined for these highly charged projectiles. A similar-size sodium cluster with a diameter of 5 nm contains approximately 1650 sodium atoms. Thus, for smaller sizes we should not expect a charge equilibration. However, for low charge state incident ions the equilibration time is expected to become smaller.

In this contribution we will describe experiments involving collisions of ions in charge states 1 to 3 with sodium clusters in the size range $n = 100$ –400. We will

^a e-mail: bhuber@cea.fr

discuss the measured charge state distributions of the residual cluster ions and their dependence on the velocity and the type of projectile. It is the aim to test whether the ionisation mechanisms discussed above do apply.

2 Experiment

The experimental set-up is described in detail in reference [11]. The principle is as follows. Neutral sodium clusters are produced in a gas aggregation source. Sodium is heated in an oven to a temperature of 350 to 400 °C. The hot sodium vapour (partial pressure ~ 0.1 mbar) expands into a cold He-atmosphere (pressure of several mbar, $T \sim 77$ K) where it condenses due to supersaturation. The formed clusters pass two differentially pumped sections before entering the interaction region, which is kept at a pressure of about 10^{-8} mbar (by using a liquid nitrogen cooled trap which encloses the extraction region). The cluster velocity depends on the cluster size and the source conditions, it ranges from 200 to 400 m/s [11]. Neutral clusters are ionised by laser irradiation (see further below) and analysed by time-of-flight mass spectrometry. The measured mass distribution follows a log-normal distribution as expected for this type of cluster source [12]. The smallest clusters contain several tens of sodium atoms, the maximum occurs at around 150 atoms with a tail reaching to clusters made of 400 atoms. The cluster density within the beam is rather low at the interaction region, integrated over the whole size distribution it amounts to about 10^5 – 10^6 clusters/cm³ [11].

The ions which are produced in a CAPRICE-ECR ion source [13] interact with the sodium clusters at the object point of a linear time-of-flight spectrometer, characterised by a mass resolution of ~ 2500 [14]. The ion beam is pulsed (10 μ s, 3 kHz) as well as the extraction field for the produced cluster ions. Intact cluster ions and charged fragments are post-accelerated to 30 kV before detection in order to obtain a comparable detection efficiency for different charge states and different masses. The particles are detected by a channelplate device and finally registered by a “multi-hit” start-stop system. This technique allowed to analyse fragmentation and fission processes and to study the correlation between several fragments. The corresponding results will be presented in a forthcoming publication [15]. Typical flight times are of the order of 100 to 200 μ s.

Under normal conditions the acquisition time for a whole spectrum amounts to approximately 4 hours. The cluster source stays operational for a period of several days before cleaning and recharging become necessary.

3 Discussion of the results

3.1 Time-of-flight mass spectra

Under similar cluster source conditions, mass spectra of ionised sodium clusters have been measured with the following projectile ions: H⁺ (5 and 20 keV); He⁺ (15 keV);

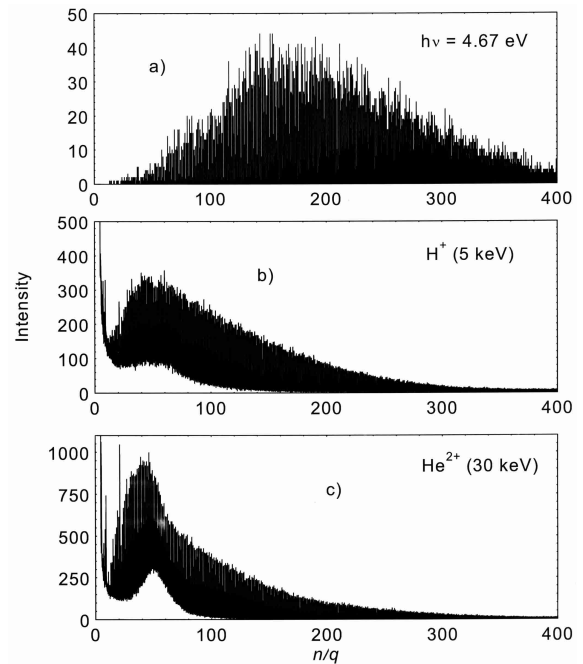


Fig. 1. Time-of-flight spectra of cluster ions transformed into spectra over n/q . (a) Ionisation by a low flux Nd-YAG laser (photon energy: 4.67 eV, flux $\sim 10 \mu\text{Joule/pulse}$); (b) spectrum obtained by 5 keV proton collisions; (c) spectrum obtained in collisions with ${}^3\text{He}^{2+}$ ions at 30 keV.

He²⁺ (30 keV) and O³⁺ (60 keV). In Figure 1 we show 3 different spectra, obtained with (a) a low-flux laser (4th harmonic of a Nd-YAG laser, $h\nu = 4.67$ eV), (b) H⁺ ions at 5 keV and (c) He²⁺ ions at 30 keV. The time-of-flight has been transformed into values of n/q (number of cluster atoms per charge state). In the first case only singly charged cluster ions are present as the laser fluence has been set to low values to avoid multi-photon absorption. Under these conditions the internal energy of the cluster is rather low (photon energy – ionisation energy < 2 eV) and can provoke at most the evaporation of one monomer, a process which requires about one eV. As the internal energy is distributed over a large system of degrees of freedom, evaporation processes are rather unlikely to occur during the experimental time scale of several μ s. The integrated mass spectrum follows a log-normal distribution $I(n) = A \exp[-(\ln(n/n_0)/\sqrt{2} \ln(\sigma))^2]$, with a maximum at $n_0 \sim 150$ and the geometric standard deviation $\sigma \sim 1.46$.

For ion-cluster collisions (Figs. 1b and 1c) the maximum of the distribution is shifted towards smaller n/q -values due to the presence of cluster ions in higher charge states. This is demonstrated in more detail in Figure 2, which shows different ranges of n/q . At $n/q \sim 200$ only singly charged ions are detected, as doubly charged ions in this range of n/q would require primary cluster sizes of about 400, where the intensity in the primary spectrum is already negligible. When the n/q -value is lower, clusters in higher charge states appear ($q = 2$ – 5). It should be noted that the peaks at integer numbers of n/q contain

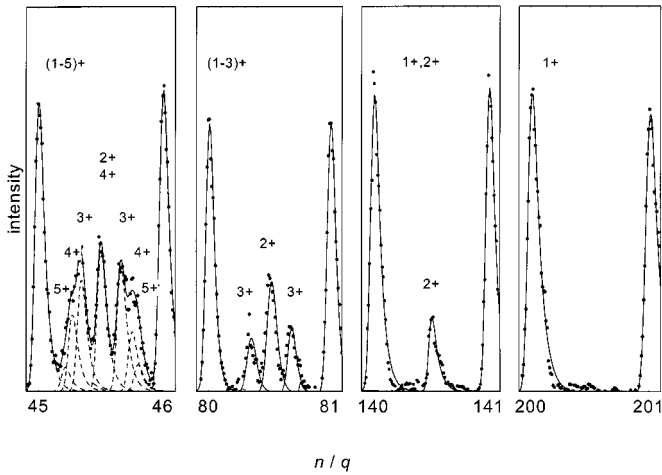


Fig. 2. Details of the spectrum at different values of n/q ($H^+ + Na_n$ at 20 keV). The dashed curves result from a deconvolution procedure.

contributions from all charge states which are present in the corresponding region. This explains the large amplitude of the integer peaks at low values of n/q (Figs. 1b and 1c) and the corresponding shift of the maximum in Figure 1 towards smaller n/q -values.

A deconvolution procedure (using asymmetric Gaussian functions [16]) reveals the mass spectra for individual charge states. In the case where several clusters of different size n and different charge q , yielding the same n/q -value, contribute to a single, a special procedure has been applied. The contribution of a given charge state is determined by averaging the intensities of neighbouring peaks of the same charge state which are well separated in flight-time. Figure 3 shows the result for 20 keV-proton collisions. The maxima of the different distributions occur at $n = 150$ – 200 with a slight tendency to increase with increasing q . At lower cluster sizes additional maxima occur and multiply charged clusters with sizes below a charge-dependent limit are absent. This phenomenon is due to the instability of multiply charged clusters below a so-called appearance size $n_{app}(q)$, which has been determined for hot sodium clusters produced by laser irradiation in charge states 2 to 5 to be 27 ± 1 , 63 ± 1 , 123 ± 2 and 206 ± 4 , respectively [17]. At smaller sizes multiply charged clusters decay by asymmetric fission processes, where small singly charged fragments Na_p^+ are emitted [15] ($p = 1$ – 5 , 7, 9, with dominant contributions from the trimer Na_3^+ and the monomer Na^+). In this process the charge state of the residual cluster is lowered by one unit and thus creates the maximum observed in the distribution of the lower charge state.

As the measured appearance size depends on the internal temperature of the produced cluster ion [15, 18, 19], we can estimate a minimum internal energy by applying the model of an evaporative ensemble [20, 21]. In this model, the fission rate k_f (or the average fission time $1/k_f$) depends on the ratio of the height of the fission barrier B_f and the internal energy E_{int} : $k_f \sim \exp(-B_f/E_{int})$. The

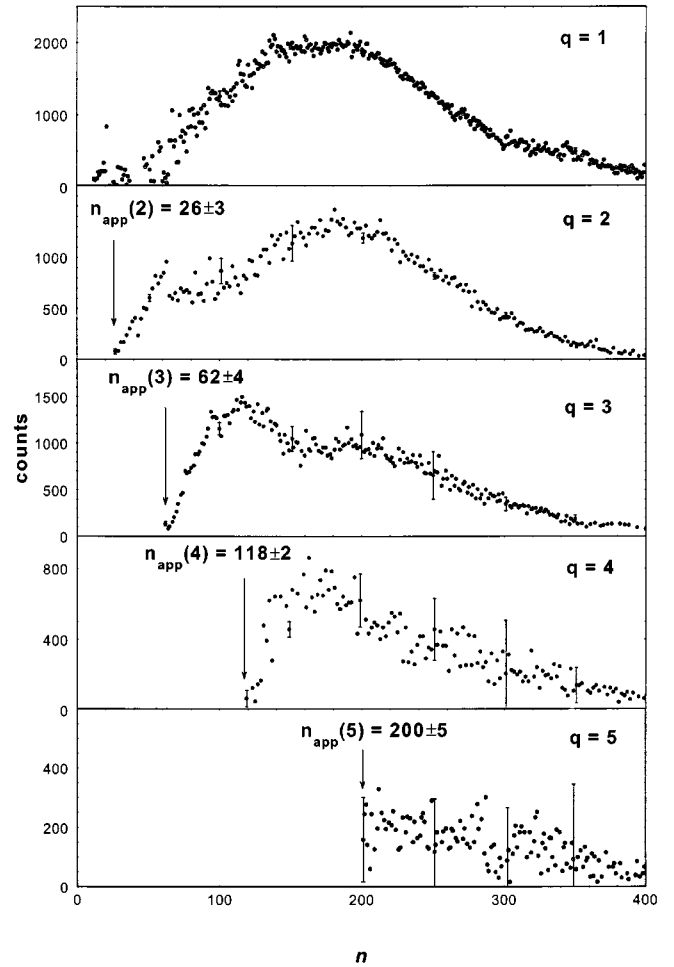


Fig. 3. Deconvoluted mass spectra of charged sodium clusters ($q = 1$ – 5). The thresholds at small cluster sizes correspond to the appearance sizes n_{app} of sodium clusters in different charge states. The error bars denote the uncertainty of the deconvolution procedure.

height of the fission barrier is calculated from a classical image charge model [22]. The appearance sizes measured for the proton impact agree within the experimental error bars with the values obtained by laser ionisation (see Fig. 3). In the latter case it has been shown that the appearance size is determined by a competition between fission and evaporation, which means, that for a system close to the appearance size the height of the fission barrier corresponds approximately to the activation energy for a monomer evaporation. For sodium clusters this is of the order of 1 eV. Equating the average fission time with the typical experimental time scale of the order of $10 \mu s$ (the sum of the ion pulse length and the average delay time between cluster ion formation and extraction), we deduce internal energies which are 2, 6, 11 and 20 eV for the “critical” systems Na_{27}^{2+} , Na_{63}^{3+} , Na_{120}^{4+} and Na_{200}^{5+} , respectively.

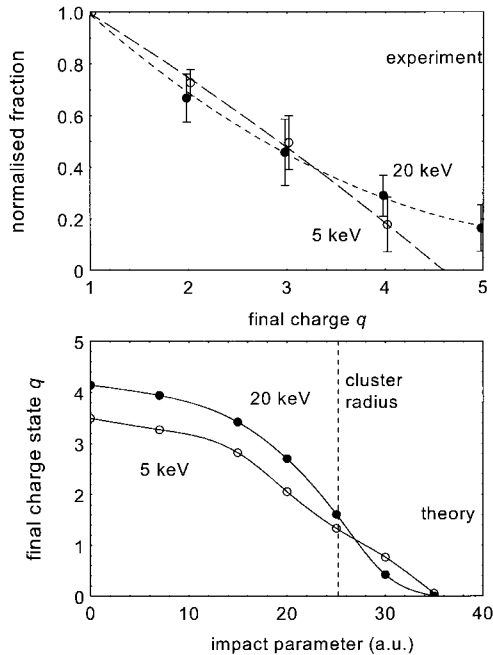


Fig. 4. Upper part: relative charge state distributions (normalised with respect to the yield of singly charged cluster ions) of Na_{220}^{q+} ions produced in collisions with H^+ projectiles at 5 keV (open circles) and 20 keV (full dots). Lower part: calculated final charge states of Na_{250}^{q+} ions as a function of the impact parameter. Collisions with H^+ projectiles at 5 keV (open circles) and 20 keV (full dots) [5].

3.2 Charge state distributions

When we neglect the importance of evaporation processes (a mass loss of several units may occur depending on the internal energy) and when we regard a size range well above the appearance size where fission is unlikely to occur, we can deduce charge state distributions for a given cluster size. In the upper part of Figure 4 the relative fraction normalised to the intensity of the singly charged cluster ions is shown for Na_{220} . Clusters are ionised in collisions with H^+ at 5 keV and 20 keV, respectively. With increasing projectile velocity multi-ionisation becomes more likely, the maximum charge state increases from 4 to (at least) 5. The lower part of Figure 4 shows predictions of a semiclassical calculation [5] concerning the final charge state as a function of the impact parameter for H^+ colliding with Na_{250} . This calculation is based on the solution of the so-called Vlasov-equation, which is the semiclassical approximation of the time-dependent Kohn-Sham equations in the local density approximation. A comparison of this semiclassical mean field theory with corresponding quantal calculations is discussed in reference [7]. The maximum charge states, which agree reasonably well with the experimental finding ($4.2 \leftrightarrow 5$, and $3.6 \leftrightarrow 4$ for 20 keV and 5 keV, respectively) are obtained in central collisions. With increasing impact parameter the trajectory inside the cluster becomes shorter and the charge state lower. When the H^+ ion passes outside of the cluster, single ionisation occurs due to single electron capture processes.

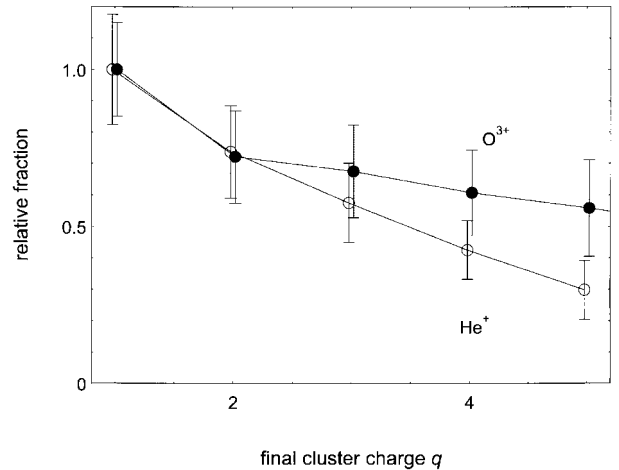


Fig. 5. Relative normalised charge state distributions of Na_{220}^{q+} clusters produced in collisions with ${}^3\text{He}^+$ ions (15 keV, $v = 0.44$ a.u.) and O^{3+} ions (60 keV, $v = 0.39$ a.u.).

The overall agreement between experiment and theory is good, in particular when we regard average charge states. At 5 keV the experimental average charge state is 1.8 ± 0.1 in agreement with the theoretical prediction, at 20 keV the experiment yields a value of 2.2 ± 0.1 , while theory gives a value of 2.4.

In Figure 5 two charge state distributions are compared for projectiles of similar velocities (~ 0.4 a.u.) but different charges. In the case of O^{3+} ions one might expect that clusters in charge states 1 to 3 should strongly dominate as they are easily produced in peripheral collisions by electron capture. However, in comparison with the He^+ projectile, the measured distribution shows a larger relative importance of cluster ions in charge states 4 and 5. This finding can be attributed to the larger energy loss of the oxygen ion when passing through the cluster, which might provoke a higher degree of ionisation.

In Figure 6 we analyse the influence of the cluster size on the multi-ionisation probability for proton- Na_n collisions (20 keV). We compare relative charge state fractions for $q = 1$ to 5. Whereas according to Figure 4 (see lower part) singly charged cluster ions are produced dominantly in peripheral collisions by electron capture, charge states $q > 1$ are mainly due to penetrating collisions. With increasing cluster size the fraction of clusters in higher charge states becomes more important, double and triple ionisation yield a lower relative fraction. This is caused by two effects: on the one hand, the ionisation potential, particularly for multi-ionisation, decreases with increasing cluster size. The total ionisation energy is given by the relation [22]: $E_{\text{ion}} = qW_b + (0.5q^2 - 0.1q)e^2/r_{\text{WS}}n^{1/3}$, where W_b corresponds to the bulk work function (0.101 a.u. or 2.74 eV for sodium), r_{WS} the Wigner Seitz radius (4 a.u. for sodium) and e the elementary charge. The energy for double ionisation of sodium cluster varies from 7.8 eV to 7.2 eV, when n is increased from 150 to 350, for 5-fold ionisation the corresponding values are 29.1 eV and 25.3 eV, respectively. On the other hand, the cluster diameter and hence the length of the trajectory inside the cluster

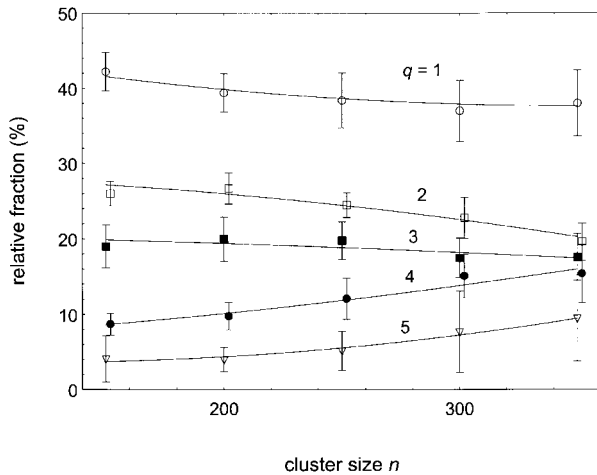


Fig. 6. Relative multi-ionisation fractions ($q = 2$ to 5) for H^+/Na_n collisions (20 keV) as a function of the cluster size n . As shown in Figure 4, these charge states are formed in penetrating collisions.

increase with $n^{1/3}$. The cluster diameters are 42.5 a.u. for Na_{150} and 56.4 a.u. for a cluster of size 350.

It should be noted that the probability for multi-ionisation increases with the velocity of the projectile, its charge state or atomic number and the length of the trajectory inside the cluster. Similar dependencies are valid for the electronic stopping of ions in solids.

3.3 Average charge state, energy loss and stopping power

According to the relation of Lindhard [1] the electronic stopping of ions in solids in the present velocity range is proportional to the velocity v , to the square of the effective charge z_{eff} and to the length of the trajectory in the target material, which in the case of clusters is proportional to $n^{1/3}$. In the upper part of Figure 7 we show the average charge state, which is defined as $\langle q \rangle = \sum qI(q) / \sum I(q)$, as a function of the product $vz_{\text{eff}}^2 n^{1/3}$. As the results correspond to proton collisions, the effective charge z_{eff} is set to 1. The averaging concerns either charge states 1 to 5 or 2 to 5, which yields a difference of about one unit. The latter case corresponds essentially to penetrating collisions, as $q = 1$ is mainly due to electron capture (see Fig. 4). Both curves increase linearly with the product of $vn^{1/3}$. It should be noted that we do not expect the curves to pass through the origin of the co-ordinate system, as the charge state 0 is not included in the averaging procedure.

In the lower part of Figure 7 we compare data for H^+ ions and He^+ ions, which have been obtained at the same velocity. Also here we find a linear increase with the product of $z_{\text{eff}}^2 n^{1/3}$. The values of z_{eff} have been determined with the TRIM-code [2] for ions passing through bulk sodium. From these findings we conclude that multi-ionisation in penetrating collisions is due to an electronic excitation, which depends on experimental parameters in the same way as the electronic stopping of ions in solids.

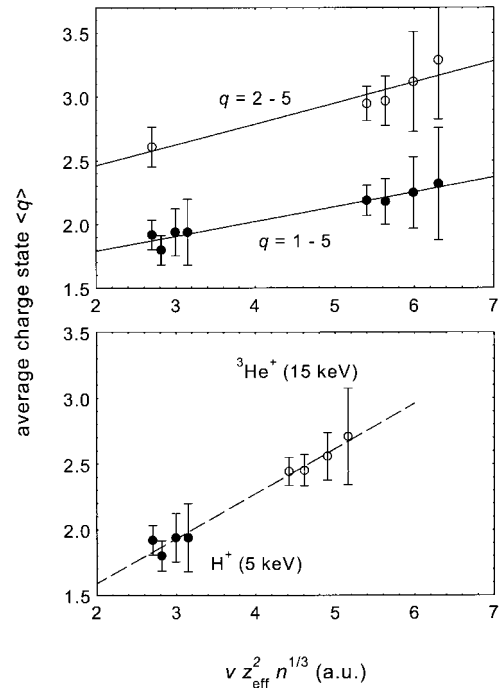


Fig. 7. Upper part: average charge state $\langle q \rangle$ of sodium clusters produced in collisions with H^+ (5 and 20 keV). Full symbols: averaging has been performed over charge states 1 to 5. Open circles: only charge states 2 to 5 have been taken into account, being representative for penetrating collisions. Lower part: average charge state $\langle q \rangle$ ($q = 1$ to 5) for collisions of H^+ and He^+ ions at a velocity of 0.4 a.u.

In order to test this relationship in a more quantitative manner, we calculated an average energy loss E_{loss} of the projectile with the aid of the TRIM-code for a typical penetrating trajectory. Averaging over all impact parameters smaller than the cluster radius R yields a mean value for the length of the penetrating trajectory of $4R/3$. Furthermore, we assume that $\langle q \rangle$ electrons will follow in first order the projectile ion with similar velocities, which yields an average kinetic energy for the accelerated electrons E_{kin} . In the case of 20 keV protons this yields a value of about 10 eV per electron. With the relation $E_{\text{loss}} = E_{\text{ion}} + E_{\text{kin}} + E_{\text{exc}}$ we can estimate the internal energy E_{exc} , which is finally stored in the vibrational modes of the ionised cluster. The result for proton collisions are shown in Figure 8 as a function of the cluster size and the projectile velocity. At 20 keV (upper part) the electronic energy loss is equally shared between the kinetic energy of the leaving electrons and the internal excitation energy. The ionisation energy is rather low. All energies increase smoothly with cluster size. The energy loss increases with the projectile velocity (lower part of Fig. 8). Whereas at low energies only a small amount is transformed into the kinetic energy of the emitted electrons, it becomes the dominant part at high energies. The average excitation energy increases from 22 eV to 29 eV when the velocity is varied from 0.4 to 0.9 a.u. These values are in very good agreement with those values which

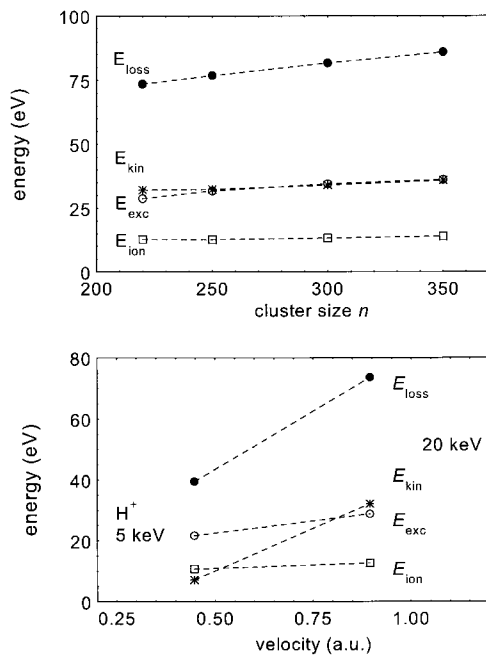


Fig. 8. Sharing of the energy loss into ionisation, kinetic and internal excitation energy. Upper part: dependence on the cluster size for 20 keV-H⁺ collisions. Lower part: variation with the projectile velocity ($n = 220$).

are necessary to explain the measured appearance sizes (see Sect. 3.1). Furthermore, they agree well with theoretical predictions which have been obtained for individual impact parameters within the semi-classical approach by solving the Vlasov equation [5].

4 Conclusion

The presented experimental results show that multi-ionisation of metal clusters in collisions with low-charged ions (H⁺, He⁺, He²⁺) is related to the electronic stopping power of these ions in the corresponding bulk material. This is in agreement with theoretical predictions [4,5] and with experimental results recently obtained in He⁺/C₆₀ collisions [23]. These experiments gave evidence that the ionisation of C₆₀-fullerenes shows the phenomenon of Z-oscillations ($Z =$ nuclear projectile charge), which is known to be a characteristic feature of the electronic stopping power in solids. The fact that in the case of sodium clusters, the measured dependencies agree with those which are valid for the electronic stopping of ions in solids, seems to indicate that the charge equilibration times are much shorter than the collision times. This is different for very highly charged projectiles, which require a time of about 7 fs [9]. A fraction of 30–50% of the energy loss is transferred into the heavy particle system favouring evaporation and fission processes. The estimated internal energies explain the large appearance sizes measured for multiply charged clusters, when they are produced in collisions with protons.

These experiments have been performed at the “Accélérateur d’Ions Multichargés AIM”, a facility of CEA Grenoble and member of the LEIF-network (HPRI-CT-1999-40012). The authors acknowledge the help of F. Gustavo in preparing the ion beams as well as fruitful discussions with L. Plagne and J. Daligault.

References

1. J. Lindhard, *Mat. Fys. Medd. Dan. Vid. Selsk.* **8**, 28 (1954).
2. J.F. Ziegler, J.P. Biersack, U. Littmark, *The stopping and Range of Ions in Solids* (Pergamon Press, New York, 1985).
3. M. Gross, C. Guet, *Z. Phys. D* **33**, 289 (1995).
4. M. Gross, C. Guet, *Phys. Rev. A* **54**, R2547 (1996).
5. L. Plagne, Ph.D. thesis, Université Joseph Fourier, Grenoble, France, 1998.
6. L. Plagne, C. Guet, *Phys. Rev. A* **59**, 4461 (1999).
7. L. Plagne, J. Daligault, K. Yabana, T. Tazawa, Y. Abe, C. Guet, *Phys. Rev. A* **61**, 033201 (2000).
8. F. Calvayrac, P.-G. Reinhard, E. Suraud, C.A. Ullrich, *Phys. Rep.* **337**, 493 (2000).
9. M. Hattass, T. Schenkel, A.V. Hamza, A.V. Barnes, M.W. Newman, J.W. McDonald, T.R. Niedermayr, G.A. Machicoane, D.H. Schneider, *Phys. Rev. Lett.* **82**, 4795 (1999).
10. R. Schlipper, R. Kusche, B.v. Issendorf, H. Haberland, *J. Appl. Phys.* (to be published).
11. T. Bergen, X. Biquard, A. Brenac, F. Chandezon, D. Jalabert, H. Lebius, M. Maurel, E. Monnard, J. Opitz, A. Pesnelle, B. Pras, C. Ristori, J.C. Rocco, B.A. Huber, *Rev. Sci. Instrum.* **70**, 3244 (1999).
12. I. Pócsik, *Z. Phys. D* **20**, 395 (1991); Y. Qiang, thesis, Albert-Ludwigs-Universität, Freiburg im Breisgau, Germany, 1997.
13. X. Biquard, A. Brenac, F. Gustavo, D. Hitz, *Rev. Sci. Instrum.* **71**, 2041 (2000).
14. F. Chandezon, B.A. Huber, C. Ristori, *Rev. Sci. Instrum.* **65**, 3344 (1994).
15. F. Chandezon, T. Bergen, A. Brenac, C. Guet, B.A. Huber, H. Lebius, A. Pesnelle, *Phys. Rev. A* **63**, 0142xx (2001).
16. The deconvolution has been performed with the programme Peak-fitTM 4.06 for Windows®, SPSS Inc. (1997).
17. T.P. Martin, U. Näher, H. Göhlich, T. Lange, *Chem. Phys. Lett.* **196**, 113 (1992); U. Näher, S. Frank, N. Malinowski, U. Zimmermann, T.P. Martin, *Z. Phys. D* **31**, 191 (1994).
18. F. Chandezon, C. Guet, B.A. Huber, D. Jalabert, M. Maurel, E. Monnard, C. Ristori, J.C. Rocco, *Phys. Rev. Lett.* **74**, 3784 (1995).
19. F. Chandezon, C. Guet, H. Lebius, A. Pesnelle, S. Tomita, B.A. Huber, *Phys. Scripta* (to be published, 2001).
20. C.E. Klots, *J. Chem. Phys.* **83**, 5954 (1985); *Nature* **327**, 222 (1987).
21. F. Chandezon, S. Bjørnholm, J. Borggreen, K. Hansen, *Phys. Rev. B* **55**, 5485 (1997).
22. U. Näher, S. Bjørnholm, S. Frauendorf, F. Garcias, C. Guet, *Phys. Rep.* **285**, 245 (1997).
23. O. Hadjar, P. Földi, R. Hoekstra, R. Morgenstern, T. Schlathölder, *Phys. Rev. Lett.* **84**, 4076 (2000).